*Clays and Clay Minerals*, Vol. 37, No. 2, 151–156, 1989.

# Mn-SUBSTITUTED GOETHITE AND Fe-SUBSTITUTED GROUTITE SYNTHESIZED AT ACID pH[1]

M. H. EBINGER AND D. G. SCHULZE

Agronomy Department, Purdue University, West Lafayette, Indiana 47907

**Abstract**—Mn-substituted iron oxides were synthesized by coprecipitating $Fe(NO_3)_3$ and $Mn(SO_4)$ solutions with $NH_4OH$, adjusting the suspensions to pH 4 or 6, and then keeping the suspensions at 55°C for 62 days. The Mn mole fraction of the final products ranged from 0 to 0.3. X-ray powder diffraction patterns showed that goethite and hematite formed in each Fe-containing system. Groutite formed in systems having initial Mn mole fractions ≥0.35. Only manganite and hausmannite formed in the pure Mn systems. The oxalate-soluble Fe in the samples increased as the Mn mole fraction increased and was slightly larger for the pH 6 series.

For samples that contained the largest Mn mole fraction, the *b* and *c* dimensions of the goethite unit cell were shifted toward those of groutite, and the *b* and *c* dimensions of the groutite unit cell were shifted toward those of goethite. Assuming the Vegard rule holds for the unit-cell *c* dimension, the goethite accommodated a maximum Mn mole fraction of 0.34, and the groutite accommodated a maximum Fe mole fraction of 0.31. The unit-cell dimensions of hematite did not vary systematically with the mole fraction of Mn in solution, probably because little Mn substituted into the hematite structure.

**Key Words**—Goethite, Groutite, Iron, Manganese, Solid solution, Synthesis, Vegard's law, X-ray powder diffraction.

## INTRODUCTION

The substitution of Al in synthetic and natural iron oxides changes their unit-cell dimensions, crystallite size, surface area, and dissolution behavior in acids (Schwertmann, 1987). Mn, like Al, occurs with Fe in many soils and sediments. The influence of Mn on the crystallization of goethite and hematite and the extent of Mn substitution into these structures is not understood completely. Karim (1984) showed that the presence of Mn lowers the crystallinity of goethite formed from slow oxidation of $FeCl_2$ solutions at pH 7. Lim-Nuñez and Gilkes (1987) showed that Mn-substituted goethites and goethites substituted with other transition metals dissolve at rates different from that of pure goethite. Stiers and Schwertmann (1985) synthesized Mn-substituted goethite and an unspecified spinel phase in 0.3 M NaOH at 60°C. Cornell and Giovanoli (1987) synthesized Mn-substituted goethite, Mn-substituted hematite, jacobsite, and a phyllomanganate at pH ≥8 and temperatures of ≥70°C. Inasmuch as many weathering reactions take place in soils at acid pH and at temperatures ≤30°C, synthesis experiments at acid pH and low temperature are needed to understand these reactions more completely.

This paper describes the chemical composition and mineralogical properties of several Fe-Mn oxyhydroxide precipitates held at acid pH and at 55°C. This temperature is lower than the temperatures used in most previous experiments and is closer to the temperatures of soils. The 55°C temperature of the synthesis is high enough, however, that sufficient quantities of goethite and hematite for analysis formed in about two months.

## MATERIALS AND METHODS

Crystalline Fe-Mn oxides and oxyhydroxides were prepared from poorly crystalline precipitates as follows. First, 120-ml volumes of 0.5 M $Fe(NO_3)_3$ and 0.5 M $MnSO_4$ were prepared having initial Mn mole fractions (Mn/(Mn + Fe)) of 0, 0.02, 0.05, 0.10, 0.20, 0.35, 0.50, and 1.00. Next, 90 ml of 2 M $NH_4OH$ was quickly added to each Fe + Mn solution; precipitates formed immediately. The suspensions were adjusted to pH 7 with 2 M $NH_4OH$ or 0.1 M $NH_4OH$ within 30 min of preparation. The precipitates were then washed three times with about 800 ml of deionized water per wash. The washed precipitates were resuspended in 1 liter of deionized water, adjusted to pH 6 (samples 3000–3100) or pH 4 (samples 4000–4100) with 1 M $HNO_3$, and kept in 1-liter polyethylene bottles at 55°C in a forced convection oven for 62 days. No further pH adjustments were made. The final products were centrifuged, washed three times with deionized water, then dried at 55°C in a forced convection oven. About 1.5 hr elapsed from the initial precipitation to the final pH adjustment, and crystal nucleation may have occurred during this time. Sulfate concentration was not determined, and some $SO_4^{2-}$ may have remained with the precipitate and could have influenced the formation of the crystalline products.

Oxalate-soluble Fe ($Fe_o$) and oxalate-soluble Mn ($Mn_o$) were determined by extracting 30-mg samples with 30 ml of pH 3 ammonium oxalate in the dark for

[1] Journal article number 11,250, Purdue Agricultural Experiment Station.

Table 1. Chemical composition and magnetic susceptibility data for the samples.

| Sample | Mole fraction Mn | | | Final pH[2] | $Fe_o/Fe_t$[3] | $Mn_o/Mn_t$[3] | $(Fe + Mn)_o/(Fe + Mn)_t$ |
|---|---|---|---|---|---|---|---|
| | Initial ppt | Final product | After oxalate[1] | | | | |
| Initial pH = 6 | | | | | | | |
| 3000 | 0 | 0 | 0 | 2.0 | 0.03 | n.d.[4] | 0.03 |
| 3002 | 0.02 | 0 | 0 | 2.3 | 0.03 | 0.02 | 0.03 |
| 3005 | 0.05 | 0.01 | 0 | 2.5 | 0.09 | 0.02 | 0.09 |
| 3010 | 0.10 | 0.01 | 0.02 | 2.4 | 0.10 | 0.11 | 0.10 |
| 3020 | 0.20 | 0.11 | n.d. | 3.0 | 0.38 | 0.18 | 0.36 |
| 3035 | 0.35 | 0.20 | n.d. | 4.0 | 0.66 | 0.51 | 0.63 |
| 3050 | 0.50 | 0.30 | n.d. | 4.8 | 0.87 | 0.71 | 0.82 |
| 3100 | 1.00 | 1.00 | n.d. | 5.2 | n.d. | 0.61 | 0.61 |
| Initial pH = 4 | | | | | | | |
| 4000 | 0 | 0 | 0 | 1.4 | 0.04 | n.d. | 0.04 |
| 4002 | 0.02 | 0 | 0 | 1.5 | 0.04 | 0 | 0.04 |
| 4005 | 0.05 | 0.01 | 0 | 1.8 | 0.04 | 0.08 | 0.04 |
| 4010 | 0.10 | 0.06 | 0.07 | 2.2 | 0.09 | 0.03 | 0.09 |
| 4020 | 0.20 | 0.14 | n.d. | 3.8 | 0.27 | 0.38 | 0.28 |
| 4035 | 0.35 | 0.18 | n.d. | 3.3 | 0.23 | 0.43 | 0.26 |
| 4050 | 0.50 | 0.28 | n.d. | 4.3 | 0.64 | 0.61 | 0.63 |
| 4100 | 1.00 | 1.00 | n.d. | 5.3 | n.d. | 0.66 | 0.66 |

[1] After 2-hr oxalate extraction.
[2] pH of sample suspension at end of the synthesis period.
[3] $Fe_o$, $Mn_o$ = oxalate soluble Fe or Mn; $Fe_t$, $Mn_t$ = total Fe or Mn.
[4] Not determined.

2 hr (Schwertmann, 1964). Total Fe ($Fe_t$) and total Mn ($Mn_t$) in the original samples and in the residue after oxalate treatment were determined on 20-mg samples dissolved in 20–25 ml of concentrated HCl. Fe and Mn were measured using a Varian Model AA-6 atomic absorption spectrophotometer.

Self-supporting mounts for X-ray powder diffraction (XRD) were prepared from samples that had been gently ground in an agate mortar. The samples were backfilled into Al sample holders and gently pressed against unglazed paper. Step-scanned XRD patterns were obtained using CoK$\alpha$ radiation (35 kV and 25 mA) and a Philips PW3100 goniometer equipped with a 1° divergence slit, a 0.2 mm receiving slit, and a graphite monochromator. Patterns of all samples were obtained from 3° to 80°2$\theta$ at 0.02° increments and counting times of 1 s per increment. Corundum (25% by weight of Buehler Micropolish, Linde C, 1.0 $\mu$m $\alpha$-$Al_2O_3$, No. 40-6310-008) was used as an internal standard for position and intensity. Additional patterns were obtained from each of the samples at 0.05° steps, 10-s counting times, and without the corundum standard. Differential X-ray powder diffraction (DXRD) patterns of samples 3050 and 4050 were obtained as described by Schulze (1981, 1986) from XRD scans collected at 0.05° steps, 50-s counting times, and without corundum.

Unit-cell *c* dimensions for goethite were calculated from the 110 and 111 line positions. Unit-cell dimensions for goethite and groutite from sample 3050 after the 2-hr oxalate treatment were calculated from the 110, 130, and 111 line positions by multiple linear regression. Other goethite and groutite lines overlapped and could not be measured accurately. Unit-cell dimensions for hematite were calculated by multiple linear regression from the 012, 110, 024, and 116 line positions. Corundum reflections near each hematite or goethite reflection were used as internal position standards for all measurements.

The mean crystallite dimensions (MCD) were calculated from the widths at half height (WHH) of the goethite 110 and hematite 012 XRD reflections. The WHH were corrected for instrumental line broadening using a novaculite standard and assuming a Cauchy line profile, and the MCD was calculated from the Scherrer equation (Klug and Alexander, 1974).

The amounts of goethite and hematite were estimated from the areas under the goethite 110 and the hematite 012 peaks. The peak areas were determined relative to the corundum 012 peak to correct for the different mass attenuation coefficients of the samples. Standard curves were prepared from mixtures of synthetic, unsubstituted goethite ($MCD_{110}$ = 170 Å) and hematite ($MCD_{012}$ = 390 Å).

Visible spectra of the dry powders were obtained with a Cary 17D spectrophotometer equipped with an integrating sphere, and Munsell color designations were calculated from the reflectance spectra as described by Fernandez and Schulze (1987).

## RESULTS AND DISCUSSION

### *Chemical properties*

The pH of the suspensions after 62 days ranged from 1.4 to 5.3 (Table 1). The pH of suspensions that con-

Table 2. X-ray powder diffraction data and Munsell color designations for goethite (Gt) and hematite (Hm) in products.

| | Cell dimensions (Å) | | | Quantities from XRD[1] (wt. %) | | MCD (nm)[2] | | Munsell color designation[3] | |
|---|---|---|---|---|---|---|---|---|---|
| | Gt | Hm | | | | | | | |
| Sample | *c* | *a* | *c* | Gt | Hm | Gt(110) | Hm(012) | Hue | Value/chroma |
| Initial pH = 6 | | | | | | | | | |
| 3000 | 3.027 | 5.044 | 13.72 | 47 | 31 | 37.4 | 52.3 | 1.8YR | 3.7/6.2 |
| 3002 | 3.027 | 5.035 | 13.77 | 32 | 43 | 26.7 | 52.3 | 1.5YR | 3.5/6.2 |
| 3005 | 3.024 | 5.035 | 13.77 | 29 | 44 | 23.4 | 40.9 | 1.9YR | 3.0/4.7 |
| 3010 | 3.019 | 5.036 | 13.77 | 10 | 64 | 20.8 | 52.3 | 1.9YR | 3.0/4.7 |
| 3020 | 3.008 | 5.041 | 13.74 | 29 | 18 | 27.5 | 52.3 | 7.7YR | 2.9/2.2 |
| 3035 | 2.993 | 5.037 | 13.78 | 16 | 7 | 26.7 | 58.8 | 8.9YR | 2.8/2.0 |
| 3050 | 2.963 | n.d.[4] | n.d. | 16 | trace | 29.2 | n.d. | 8.5YR | 2.7/1.7 |
| 3100 | n.d. | n.d. | n.d. | 0 | 0 | n.d. | n.d. | 9.4YR | 4.7/4.2 |
| Initial pH = 4 | | | | | | | | | |
| 4000 | 3.026 | 5.042 | 13.75 | 11 | 70 | 15.3 | 52.3 | 1.0YR | 3.3/6.1 |
| 4002 | n.d. | 5.046 | 13.75 | 5 | 74 | 8.9 | 49.5 | 0.9YR | 3.1/5.8 |
| 4005 | 3.025 | 5.039 | 13.76 | 25 | 49 | 18.7 | 34.9 | 1.9YR | 3.2/2.6 |
| 4010 | 3.017 | 5.038 | 13.75 | 40 | 22 | 24.6 | 72.4 | 7.7YR | 3.2/2.6 |
| 4020 | 3.001 | n.d. | n.d. | 21 | 7 | 26.7 | 24.8 | 8.6YR | 2.7/1.8 |
| 4035 | 2.991 | 5.040 | 13.79 | 20 | 14 | 26.0 | 37.6 | 9.2YR | 2.9/1.6 |
| 4050 | 2.983 | n.d. | n.d. | 19 | 3 | 31.2 | n.d. | 8.8YR | 2.6/1.6 |
| 4100 | n.d. | n.d. | n.d. | 0 | 0 | n.d. | n.d. | 9.4YR | 4.6/3.7 |

[1] From goethite 110 and hematite 012 X-ray powder diffraction line intensities. Sum of Gt + Hm + oxalate soluble material (Table 1) does not necessarily equal 100% because Gt and Hm standards did not contain Mn and had smaller MCD values than the samples. Additional error is due to coincident 110 reflections of goethite and groutite.

[2] Mean crystallite dimension calculated from widths at half height of goethite (110) and hematite (012) reflections.

[3] Calculated from reflectance spectra.

[4] Not determined.

tained no Mn decreased the most. The pH of sample 3000 decreased from 6 to 2, and that of sample 4000, from 4 to 1.4. The pH of suspensions having larger Mn mole fractions decreased the least. The pH of sample 3050 decreased from 6 to 4.8, and that of sample 4050 increased from 4 to 4.3. The pH of suspensions having the lowest Mn mole fraction decreased the most because hydrolysis of $Fe^{3+}$ releases three protons, compared with the hydrolysis of $Mn^{2+}$ which releases only two protons (Lindsay, 1979). The suspensions were not well buffered, thus, a small increase in the $H^+$ activity resulted in a large decrease in pH.

The Mn mole fraction of the solid products after 62 days was less than the Mn mole fraction of the initial solutions (Table 1). The supernatants were not analyzed, but some Mn was probably lost when the initial precipitates and the final products were washed.

The products having the greatest Mn content had the largest oxalate solubilities (Table 1). The ratio of oxalate-soluble Mn to total Mn ($Mn_o/Mn_t$) was generally greater than the $Fe_o/Fe_t$ ratio for samples of the 4000 series, but this trend was reversed for samples of the 3000 series. The $(Fe + Mn)_o/(Fe + Mn)_t$ ratio was slightly greater for samples of the 3000 series than for samples of the 4000 series. The presence of ferrihydrite was suggested by the relatively large $(Mn + Fe)_o/(Mn + Fe)_t$ ratios of the samples that contained Mn. The actual ferrihydrite content, however, may be lower than that indicated by $(Mn + Fe)_o/(Mn + Fe)_t$ ratios because both ferrihydrite and crystalline Mn oxides are soluble in acidified ammonium oxalate (Chao and Theobald, 1983). Cornell and Giovanoli (1987) also found that solubility in acid ammonium oxalate does not reliably measure the extent of poorly crystalline-to-crystalline mineral transformation if Mn oxides are present. The pure Mn samples (samples 3100 and 4100) dissolved completely during the oxalate extraction, but a white solid precipitated before the extracts were analyzed for Mn. Thus, the oxalate ratio for these two samples was $<1.0$ (Table 1). The XRD pattern of the white precipitate matched the patterns of Mn oxalate and Mn oxalate dihydrate (ASTM, 1964). No precipitates were observed in the extracts from samples containing both Fe and Mn.

### *X-ray powder diffraction*

Hausmannite ($Mn_3O_4$) and manganite ($\gamma$-MnOOH) were identified in samples 3100 and 4100. These two samples contained only Mn and were the only samples that contained hausmannite and manganite. Goethite and hematite were present in different amounts in all the other samples (Table 2). More goethite and less hematite were present in samples of the 3000 series than in samples of the 4000 series, probably because of the different initial pH. Schwertmann and Murad (1983) showed that the goethite/hematite ratio in a synthetic system that contained only Fe was greatest at pH 1 to 4 and at pH 9 to 12. Trends in goethite/

https://doi.org/10.1346/CCMN.1989.0370206 Published online by Cambridge University Press

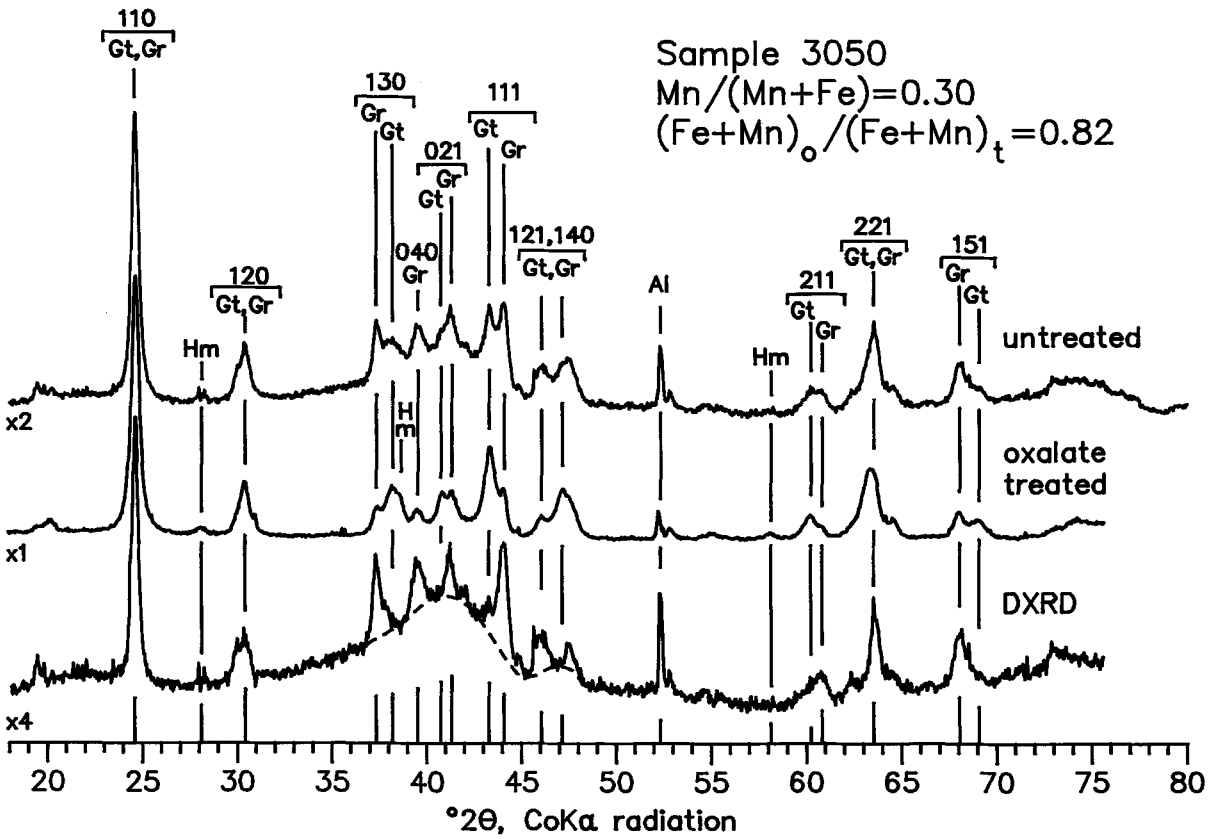


Figure 1. Slow step-scanned X-ray powder diffraction patterns of sample 3050 before and after oxalate treatment, and differential X-ray powder diffraction pattern obtained by subtracting the pattern of oxalate-treated material from that of the untreated material. ×1, ×2, and ×4 denote relative scale expansion. Gt = goethite, Gr = groutite, Hm = hematite, Al = Al metal from edge of sample holder. Gt, Gr = Gt and Gr peaks are not resolved. Dashed line delineates the broad ferrihydrite peak.

hematite ratios from either the pH 6 or pH 4 data of the present study, however, cannot be related directly to pH or Mn addition, because the pH was not controlled or measured after the initial adjustment. The mean crystallite dimensions (MCD) of the goethite 110 XRD reflection decreased as the goethite content decreased (Table 2). A similar trend was shown by Schwertmann and Murad (1983).

Groutite, $\alpha$-MnOOH, was present in samples 3050 and 4050 as indicated by clearly resolved 130, 021, 111, 211, and 151 XRD reflections (Figure 1). Groutite partially dissolved after the 2-hr oxalate treatment, as shown by the decrease in the intensity of its XRD reflections. Groutite reflections were clearly resolved in the DXRD pattern, even though groutite and goethite reflections were coincident in the patterns from the untreated sample and in the pattern of the sample treated for 2 hr with oxalate. The groutite dissolved completely after an additional 4-hr oxalate treatment (data not shown). The presence of groutite is suggested in samples 3035, 4020, and 4035 by unresolved shoulders on the goethite 130 and 111 XRD lines, corresponding to the groutite 130 and 111 reflections (data not shown). The broad peak between 35° and 45°2$\theta$ (centered at 2.556 Å) and the smaller peak between 45° and 48°2$\theta$ (centered at 2.268 Å) in the DXRD pattern correspond to the ferrihydrite 110 and 112 XRD lines (dashed line, Figure 1).

Table 3. Unit-cell dimensions (Å) of pure goethite and groutite and of goethite and groutite in sample 3050 after 2-hr oxalate treatment.

| Sample | *a* | *b* | *c* |
|---|---|---|---|
| Goethite (JCPDS Card 29-713*) | 4.608 | 9.956 | 3.0215 |
| Goethite in sample 3050 | 4.607 | 10.06 | 2.963 |
| Groutite in sample 3050 | 4.541 | 10.57 | 2.905 |
| Groutite (JCPDS Card 12-733i) | 4.565 | 10.699 | 2.852 |

The *c* dimension of goethite decreased as the Mn mole fraction increased and was intermediate between goethite and groutite (Tables 2 and 3). $Fe^{3+}$ and $Mn^{3+}$ have ionic radii of 0.645 Å and 0.65 Å, respectively (Shannon and Prewitt, 1969), but $Mn^{3+}$ has one less *d*

https://doi.org/10.1346/CCMN.1989.0370206 Published online by Cambridge University Press

electron than $Fe^{3+}$. This electron deficiency causes a Jahn-Teller distortion in the $Mn^{3+}$ octahedron (Burns, 1970) that shortens the four equatorial Mn–O bonds and elongates the two axial Mn–O bonds (Dent-Glasser and Ingram, 1969). This distortion decreases the *a* and *c* dimensions of the unit cell, but increases the *b* dimension (Stiers and Schwertmann, 1985). Thus, the smaller *c* dimensions of the samples having the largest Mn mole fractions indicate that $Mn^{3+}$ substituted for $Fe^{3+}$ in the goethite structure.

Sample 3050 contained only a trace of hematite, and the XRD reflections of both goethite and groutite were large enough to be measured accurately. The unit-cell dimensions of goethite and groutite were compared with the cell dimensions of goethite and groutite listed in the JCPDS (1980) card file (Table 3). The groutite unit-cell dimensions correctly predicted the positions of the remaining groutite lines in the DXRD pattern of Figure 1. The *b* and *c* dimensions of the goethite and groutite in sample 3050 were between the *b* and *c* dimensions of the goethite and groutite given in the JCPDS (1980) files, suggesting that the goethite contained $Mn^{3+}$ and that the groutite contained $Fe^{3+}$.

Schulze (1984) showed that Vegard's rule closely predicted the changes in the *b* and *c* dimensions of goethite as $Al^{3+}$ substitution increased, but that it did not predict the *a* dimension because of the influence of structural defects. If Schulze's (1984) conclusion holds for a solid solution of goethite and groutite, the *b* and *c* dimensions of goethite and groutite should also predict the Mn substitution. For goethite in sample 3050, Vegard's rule predicted 0.14 Mn mole fraction from the *b* dimension and 0.34 Mn mole fraction from the *c* dimension. For groutite in sample 3050, Vegard's rule predicted 0.83 Mn mole fraction (0.17 Fe mole fraction) from the *b* dimension and 0.69 Mn mole fraction (0.31 Fe mole fraction) from the *c* dimension. The *a* dimension of the goethite was between the *a* dimensions of goethite and groutite listed in the JCPDS (1980) file, but the *a* dimension of the groutite was considerably smaller than that of groutite listed in the file. Why the *a* dimension of the Fe-substituted groutite was so small is not known. The *a* dimension may have been influenced by structural defects as it is in Al-substituted goethite (Schulze, 1984). A complete solid solution between groutite and goethite may exist because $Mn^{3+}$ substituted for $Fe^{3+}$ in goethite and $Fe^{3+}$ substituted for $Mn^{3+}$ in groutite. The goethite structure, however, appears to tolerate a maximum of about 0.33 mole fraction Al substitution (Schwertmann, 1987).

All the XRD reflections of Al-substituted goethite shifted to higher angles (i.e., smaller d-values) relative to pure goethite, because all the unit-cell dimensions of goethite decrease as a result of Al substitution (Schulze, 1984). In contrast, Mn substitution in goethite caused the *a* and *c* dimensions to decrease, but the *b* dimension to increase. Thus, the XRD reflections of Mn-substituted goethite shifted in different directions, depending on their Miller indices. For example, the 110 reflections of goethite and groutite were coincident, the 130 reflection of groutite was at a lower angle (larger d) than the 130 reflection of goethite, but the 111 reflection of groutite was at a *higher* angle (i.e., smaller d) than the 111 reflection of goethite (Figure 1). The complex line shifts would make XRD identification of Mn-substituted goethite or Fe-substituted groutite in natural samples difficult without careful analysis of the data.

The *a* and *c* dimension of the synthetic hematite did not change systematically with the Mn mole fraction (Table 2), and were similar to the *a* and *c* dimensions given for hematite on JCPDS card 24-72 ($a$ = 5.038 Å, $c$ = 13.772 Å). The lack of systematic variation in the hematite unit-cell dimensions made it difficult to determine if Mn substituted into the hematite structure. Cornell and Giovanoli (1985) showed that Mn inhibited the formation of hematite unless oxalate anion was present in the system. They reported as much as 0.05 mole fraction Mn in the hematite that formed from an oxalate-containing system. The data from the present investigation suggest that no Mn substituted into the hematite structure.

### *Color*

The colors of the samples fell into two major groups. Samples that had low Mn mole fractions (samples 3000 to 3010 and 4000 to 4005) were moderate reddish brown with hues of 0.9YR to 1.9YR, values of 3.0 to 3.7, and chromas of 4.7 to 6.2 (Table 2). The reddish brown hues were due to the relatively large amounts of hematite in these samples. A second group consisted of the Fe-containing samples having the highest Mn mole fractions. Samples 3035, 3050, 4020, 4035, and 4050 were dark grayish yellowish brown and had hues of 8.5YR to 9.2YR, values of 2.6 to 2.9, and chromas of 1.6 to 2.0 (Table 2). These samples were yellower and darker than the samples that contained less Mn. The colors of samples 3020 and 4010 were intermediate between these two groups, and the pure Mn samples were moderate yellowish brown (9.4YR 4.6/4.0). The dark colors of the Mn-substituted goethite and Fe-substituted groutite would make it difficult to distinguish these minerals visually from other dark-colored Mn minerals.

## SUMMARY AND CONCLUSIONS

Goethite, groutite, hematite, and ferrihydrite formed from mixed Fe-Mn coprecipitates adjusted to an initial pH of 4 or 6 and kept at 55°C for 62 days. Changes in the unit-cell dimensions showed that Mn substituted into the goethite structure and Fe substituted into the groutite structure, but no clear evidence for Mn substitution in hematite was found. The effect of pH on

phase transformations and on the amount of Mn incorporated into the phases that formed could not be clearly determined, because the pH was not controlled during the experiment. The two suspensions that contained the largest amounts of groutite, however, had the smallest changes in pH during the experiment. Thus, pH between 4 and 6 was probably favorable for the formation of Mn-substituted goethite and Fe-substituted groutite. Identification of Mn-substituted goethite or Fe-substituted groutite in natural samples would require careful analysis of XRD data to detect the complex shifts in the XRD reflections that indicate the presence of these phases.

## ACKNOWLEDGMENTS

We thank the USDA-ARS, National Soil Erosion Laboratory for the use of the X-ray diffractometer and U. Schwertmann, J. L. White, and J. L. Alrichs for critical reviews of the manuscript.

## REFERENCES

ASTM (1964) *Index to the Powder Diffraction File: ASTM Special Technical Publication 48-M1,* ASTM, Philadelphia, p. 326.

Burns, R. G. (1970) *Mineralogical Applications of Crystal Field Theory:* Cambridge University Press, Cambridge, 106–127.

Chao, T. T. and Theobald, P. K. (1983) The significance of iron and manganese oxides in geochemical exploration: *Econ. Geol.* **71,** 1560–1569.

Cornell, R. M. and Giovanoli, R. (1987) Effect of manganese on the transformation of ferrihydrite into goethite and jacobsite in alkaline media: *Clays & Clay Minerals* **35,** 11–20.

Dent-Glasser, L. S. and Ingram, L. (1969) Refinement of the crystal structure of groutite, $\alpha$-MnOOH: *Acta Crystallogr.* **B24,** 1233–1236.

Fernandez, R. N. and Schulze, D. G. (1987) Calculation of soil color from reflectance spectra: *Soil Sci. Soc. Amer. J.* **51,** 1277–1282.

JCPDS (1980) *Mineral Powder Diffraction Files: Data Book:* JCPDS International Center for Diffraction Data, Swarthmore, Pennsylvania.

Karim, Z. (1984) Influence of transition metals on the formation of iron oxides during the oxidation of $Fe(II)Cl_2$ solution: *Clays & Clay Minerals* **32,** 334–336.

Klug, H. P. and Alexander, L. E. (1974) *X-ray Diffraction Procedures for Polycrystalline and Amorphous Materials:* Wiley, New York, 966 pp.

Lim-Nuñez, R. and Gilkes, R. J. (1987) Acid dissolution of synthetic metal containing goethites and hematites: in *Proc. Int. Clay Conf., Denver, 1985,* L. G. Schultz, H. van Olphen, and F. A. Mumpton, eds., The Clay Minerals Society, Bloomington, Indiana, 187–204.

Lindsay, W. L. (1979) *Chemical Equilibria in Soils:* Wiley, New York, 449 pp.

Schulze, D. G. (1981) Identification of soil iron oxide minerals by differential X-ray diffraction: *Soil Sci. Soc. Amer. J.* **45,** 437–440.

Schulze, D. G. (1984) The influence of aluminum on iron oxides. VIII. Unit-cell dimensions of Al-substituted goethite and estimation of Al from them: *Clays & Clay Minerals* **32,** 36–44.

Schulze, D. G. (1986) Correction of mismatches on $2\theta$ scales during differential X-ray diffraction: *Clays & Clay Minerals* **34,** 681–685.

Schwertmann, U. (1964) Differenzierung der Eisenoxide des Bodens durch Extraktion mit einer Ammoniumoxalatlösung: *Pflanzenernaehr. Bodenkd.* **105,** 194–202.

Schwertmann, U. (1987) Some properties of soil and synthetic iron oxides: in *Iron in Soils and Clay Minerals, Proc. of NATO Adv. Study Inst.,* J. W. Stucki, B. A. Goodman, and U. Schwertmann, eds., D. Reidel, Boston, 203–250.

Schwertmann, U. and Murad, E. (1983) Effect of pH on the formation of goethite and hematite from ferrihydrite: *Clays & Clay Minerals* **31,** 277–284.

Shannon, R. D. and Prewitt, C. T. (1969) Effective ionic radii in oxides and fluorides: *Acta Crystallogr.* **B25,** 925–946.

Stiers, W. and Schwertmann, U. (1985) Evidence for manganese substitution in synthetic goethite: *Geochim. Cosmochim. Acta* **49,** 1909–1911.

*(Received 10 August 1987; accepted 17 October 1988; Ms. 1707)*